Decentralized Inverter Control with Selective Harmonic Damping Connected to a Multi-Bus Grid

T. S. Amorim, D. Carletti, W. N. Sepulchro, L. F. Encarnação

***Abstract*—The increasing use of non-linear loads and distributed generation units in distribution system raises the grids' harmonic content. One way to mitigate harmonics is to employ active power filters, which can be added to already-existing DG controls. Thus, in addition to contributing to grid voltage regulation and frequency stability, DGs could also mitigate voltage and current harmonics. The proposed selective and decentralized harmonic damping control with adaptive gain is applied to eight grid-connected inverters in a modified IEEE 33-bus system. To evaluate the effectiveness of the suggested control against variations in the system's power flow, the modified IEEE 33-bus system is set up in two different topologies. A Modulated Model Predictive Control (M2PC) is applied to the current control loop in the grid-tied inverter with an L filter. To verify the effectiveness of the control strategy proposed in this work, simulations were carried out on a real-time simulation platform.**

***Keywords*: distributed generation, distribution system, grid-tied inverter, harmonic compensation, voltage regulation.**

I. Introduction

With the increasing use of non-linear loads in the distribution system, power quality problems, such as harmonics generated by non-linear loads, flow of harmonic currents and the increase in voltages caused by harmonics, are becoming a concern in electrical systems [1][2]. This problem is particularly concerning in low voltage distribution systems, where equipment such as computers and fluorescent lamps, for example, have a direct impact on distribution systems and have undesirable effects on network parameters and system reliability [2][3]. Distorted bus voltages and line currents can lead to excessive losses, poor power transfer, and low power factor. Furthermore, harmonic distortion can reduce the lifespan of electrical system equipment, such as transformers, power factor correction capacitors, and induction motors [4]. These harmonic voltages can also affect sensitive loads or interfere with communication systems close to the power system infrastructure [2].

The traditional way to mitigate harmonics is to use passive filters or centralized active power filters. In addition to requiring additional investment from the utility, they are not very effective in low voltage distribution systems, since in these systems the loads are highly distributed. In this case, distributed active power filters would be a better solution [2].

With increasing concerns about energy cost, the environment and energy security, more distributed generation (DG) units based on renewable energy sources (RES) are being connected to the distribution system. These DGs are normally connected to the grid through power electronics-based devices with output filters [2]. Problems related to power quality become more relevant with the increasing penetration of DG units in the electrical system. Although the integration of static converters based on power electronics and non-linear loads can deteriorate power quality, the use of multifunctional DGs is an option for improving the power quality of an electrical system [3]. Inverters used to interface RES with the electrical system, if properly controlled, can provide several ancillary services, such as compensation of harmonic voltages and currents, and, consequently, can improve power quality [1].

Considering that RES-based DGs, such as photovoltaic and wind systems, do not always operate at nominal power, the residual capacity of DGs can be used to provide ancillary services without additional costs. Furthermore, these interface converters can respond quickly with digital controller and voltage and current feedback measurement. Thus, the use of DG units with a converter-based interface is feasible to improve the electrical energy quality of a distribution system [2].

Selective compensation for some power quality problems, such as load asymmetry, harmonics, and reactive power, can reduce voltage unbalance and harmonic distortion and improve the use of the distribution infrastructure, allowing the system's power capacity to be increased [5].

On the other hand, the high penetration of DGs, in addition to contributing to the proliferation of harmonic currents and voltages, also has the disadvantage of not presenting inertial behavior, which can become a problem in relation to system stability [6]. These DC-AC converters usually have instantaneous constant power controls, called PQ Control, or similar control strategies [7].

In the electrical system, the frequency of the generated voltage is stabilized by the combination of the rotational inertia of synchronous generators and controllers that act on the rotational speed of these synchronous generators. Therefore, the replacement of a significant part of the synchronous generation with non-rotational generation units results in a reduction in the total inertia of the system, harming the angular and frequency stability of the electrical systems. A solution proposed in the

This work was supported by the National Council for Scientific and Technological Development—CNPq (grant numbers 404857/2023-0 and 311848/2021-4) and Espírito Santo Research and Innovation Support Foundation—FAPES (grant number 1024/2022).

T. S. Amorim, W. N. Sepulchro, and L. F. Encarnação are with Federal University of Espírito Santo, Vitoria, ES 29075910 Brazil (e-mail of corresponding author: thiago.s.amorim@ufes.br).

D. Carletti is with Instituto Federal do Espírito Santo, São Mateus, ES 29932540 Brazil.

Paper submitted to the International Conference on Power Systems Transients (IPST2025) in Guadalajara, Mexico, June 8-12, 2025.

literature to increase system stability is to make the distributed generation combined with an interface inverter behave like a synchronous machine (SM). This can be achieved by properly controlling the inverter power. Thus, controls called virtual synchronous generator (VSG) were proposed in the literature, which emulate the inertial characteristic and damping of electromechanical oscillations common to physical synchronous machines [8][9].

The control strategies to manage several devices to mitigate harmonic voltages and currents can be centralized, decentralized, distributed, hybrid, and flexible [10].

Decentralized controls [11]-[13] measure only local voltages and currents in order to calculate the reference signals control of power electronics devices. The application of decentralized control is feasible in grids which don't have a suitable communication network due to its high installation cost. Although this control is not complex, the improvement of harmonic distortion at the point where the inverter is connected can lead to deterioration of harmonic content at other points in the system, known as the whack-a-mole effect. Centralized controls [14][15] have a central controller that shares information with local controllers through unidirectional or bidirectional communication channels. The multifunctional inverters' coordinated operation is guaranteed by the central controller. However, electrical systems with high penetration of multifunctional inverters may demand high computational cost of the central controller and complex communication networks. Failures in communication networks, long time delay and limits on system expansion are problems that can make it difficult to implement centralized controls in an electrical system. Distributed controls [10], [16]-[18] have a reduced communication network and share information between the inverters in the system. This makes it possible to share tasks between them, such as sharing power and harmonic mitigation. This type of control avoids some problems caused by using centralized controls, such as lack of reliability and security, and decentralized controls, such as the non-use of an existing communication structure and the whack-a-mole effect. Hybrid controls combine features of two controls strategies in a single controller, such as the control proposed in [19], which combines features of centralized and distributed controls. Flexible controls have characteristics of two controls in a single controller, but these controls do not work simultaneously, like the control proposed in [20], which can act as a centralized or decentralized control.

The application of inverters with decentralized control would be the best option for existing electrical systems that do not have central controls, since communication networks have a high installation cost. This control does not use unidirectional or bidirectional communication channels between the grid-tied inverter and a central control or between grid-tied inverters on the same grid, as in centralized and distributed controls, respectively.

The proposal of this work is to simultaneously implement harmonic voltage damping and virtual inertia controls in eight inverters connected to the modified IEEE 33-bus system [21]. A decentralized control structure is employed because the system under study lacks an existing communication network. This control structure solely measures the voltage at the DG bus. Selective control compensates only for the dominant harmonics in distribution systems and the gain of each harmonic frequency is adaptive. Two configurations of the modified IEEE 33-bus system are included to test whether the suggested control functions as intended in situations where the system's power flow changes. The system will be simulated in a setup with Texas Instruments' digital signal processor (DSP) TMSF28379D connected to Typhoon HIL's HIL602 modules through Typhoon HIL's HIL TI DSP 180 Interface Card. Simulations are performed to verify that the proposed decentralized control can dampen harmonics and support the system voltage even in cases where there is power flow inversion and can minimize the whack-a-mole effect that may occur due to the lack of a central system to control the inverters.

The rest of this paper is structured as follows. The VSG model utilized in DG control is presented in Section II. The *p-q* Theory-based decentralized and selective control for dampening harmonic voltages is shown in Section III. Section IV presents the modified IEEE 33-bus system in which the DGs with the proposed control were installed and the system implementation details on the real-time simulation platform composed of four HIL602 devices and four DSP TMSF28379D. In section V, the results of real-time simulation with the modified IEEE 33-bus system are presented to verify the effectiveness of the proposed control. Section VI shows the conclusions of this work. Communication-based solutions are outside the scope of this work.

II. VIRTUAL SYNCHRONOUS GENERATOR

The idea of control with virtual inertia is to mimic the behavior of a SM, especially in relation to the emulation of mechanical characteristics of these machines, so that the DC-AC interface converter that connects the non-inertial source to the electrical system has a behavior like a SM in the occurrence of disturbances in the electrical system. Therefore, the basic principle of any inertial control strategy is based on the implementation of the swing equation of a SM. Equations (1) and (2) present the complete mechanical modeling for a SM [7].

$$T_m - T_e - D\cdot\Delta\omega = \frac{P_m}{\omega} - \frac{P_e}{\omega} - D\cdot\Delta\omega = J\frac{d\omega}{dt} \quad (1)$$

$$\frac{d\theta}{dt} = \omega \quad (2)$$

Where T_m is the mechanical torque, T_e is the electrical torque, P_m is the mechanical power, P_e is the electrical power, ω is the angular velocity, $\Delta\omega$ is the angular velocity deviation, θ is the rotor angle, D is the mechanical damping coefficient, and J is the virtual moment of inertia.

The simplified model of the VSG used in this work is based on the model presented in [22]. A three-phase SM model is used to calculate reference currents, and the three-phase model reproduces the MS stator circuit and mechanical subsystem. In place of a field circuit, an adjustable induced voltage in the stator is considered. The VSG reference current, $\vec{i}^{*}_{VSG} = [i_{VSG,a} \quad i_{VSG,b} \quad i_{VSG,c}]^T$, is calculated by Equation (3).

$$\vec{i}^{*}_{VSG} = (\vec{e} - \vec{v}_{PCC1+})/(R_{VSG} + L_{VSG}s) \quad (3)$$

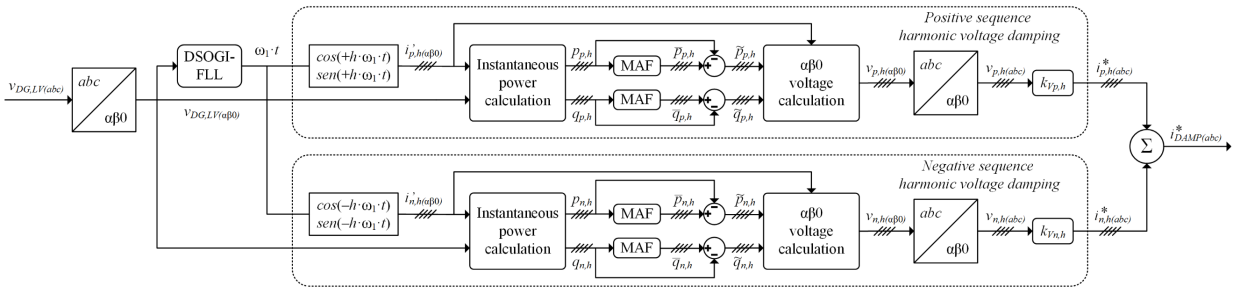

Fig. 1 - Decentralized and selective control with adaptive gain for damping of harmonic voltages, h = 5th, 7th, 11th, and 13th

Where $\vec{e} = [e_a \quad e_b \quad e_c]^T$ is the induced electromotive force (EMF), $\vec{v}_{PCC1+} = [v_{PCC1+,a} \quad v_{PCC1+,b} \quad v_{PCC1+,c}]^T$ is the fundamental component positive sequence of the voltage at the point of common coupling (PCC) and is tracked with a dual second order generalized integrator - frequency-locked loop (DSOGI-FLL) [23], R_{VSG} and L_{VSG} are the stator resistance and inductance, respectively.

The induced EMF is determined by Equation (4).

$$\vec{e} = E_p[\sin(\theta) \quad \sin(\theta - 2\pi/3) \quad \sin(\theta + 2\pi/3)]^T \qquad (4)$$

Where E_p is the induced EMF adjustable amplitude calculated by Equation (5).

$$E_p = E^* + (Q^* - Q)\left(K_{pQ} + K_{iQ}/s\right) \qquad (5)$$

Where E^* is the reference induced EMF, Q^* is the reactive power reference, Q is the inverter reactive power, K_{pQ} and K_{iQ} are the PI controller proportional and integral gains, respectively.

III. Selective Harmonic Detection with Adaptive Gain

The use of harmonic voltage damping controls is more suitable for improving the overall power quality of the electrical system, since this control does not compensate for specific system loads and the harmonic voltage detected at a given point in the system is the result of the various harmonic loads connected to the grid and voltage drops across the system impedances. The proposed harmonic damping controller is *p-q* Theory-based [24] and measures only the three-phase DG voltages at the PCC ($v_{DG,LV(abc)}$) to compensate for the 5th, 7th, 11th, and 13th harmonics, which are the background dominant harmonics in distribution networks. Positive and negative sequence harmonic auxiliary currents ($i'_{p,h(\alpha\beta0)}$ e $i'_{n,h(\alpha\beta0)}$, respectively) are generated from the angle tracked by DSOGI-FLL ($\omega_1 \cdot t$), and these currents are used to calculate the harmonic auxiliary positive and negative sequence active ($p_{p,h}$ and $p_{n,h}$) and imaginary powers ($q_{p,h}$ and $q_{n,h}$), respectively). The constant positive and negative sequence active ($\bar{p}_{p,h}$ and $\bar{p}_{n,h}$, respectively) and imaginary powers ($\bar{q}_{p,h}$ and $\bar{q}_{n,h}$, respectively) required to extract the positive and negative sequence harmonic voltages from the DG voltage at the PCC ($v_{p,h(\alpha\beta0)}$ and $v_{n,h(\alpha\beta0)}$, respectively) are extracted using a moving average filter (MAF). The positive and negative sequence DG harmonic voltages at the PCC at *abc*-axis ($v_{p,h(abc)}$ and $v_{n,h(abc)}$, respectively) are determined using the inverse Clarke transform. Positive and negative sequence adaptive harmonic gains ($k_{Vp,h}$ and $k_{Vn,h}$, respectively) are used to determine the compensating harmonic currents. The calculation of the reference current (i^*_{DAMP}) of the harmonic detection circuit is given by Equation (6) and Fig. 1 shows the block diagram of the proposed harmonic damping strategy.

$$i^*_{DAMP} = \sum_{h=5,7,11,13} k_{Vp,h} \cdot v_{p,h} + k_{Vn,h} \cdot v_{n,h} \qquad (6)$$

The proposed adaptive gain is updated (T_u) every 0.2 s [25] from the error of the positive and negative sequence voltages at instants k and k–1. The deviations of the positive and negative sequence harmonic voltages are calculated according to Equations (7) and (8).

$$\varepsilon_{Vp,h} = V_{PCCp,h}(k) - V_{PCCp,h}(k-1) \qquad (7)$$

$$\varepsilon_{Vn,h} = V_{PCCn,h}(k) - V_{PCCn,h}(k-1) \qquad (8)$$

Where $V_{PCCp,h}(k–1)$ are $V_{PCCn,h}(k–1)$ are the the positive and negative sequence components amplitudes of the PCC voltage at instant k–1, respectively, and $V_{PCCp,h(k)}$ and $V_{PCCn,h(k)}$ are the positive and negative sequence components amplitudes of the PCC voltage at instant k, respectively.

The adaptive positive and negative sequences gains at instant k ($k_{Vp,h}(k)$ and $k_{Vn,h}(k)$, respectively) used in this work are calculated according to (9) and (10), respectively.

$$k_{Vp,h}(k) = k_{Vp,h}(k-1) + \Delta k_{V,h}\varepsilon_{Vp,h} \qquad (9)$$

$$k_{Vn,h}(k) = k_{Vn,h}(k-1) + \Delta k_{V,h}\varepsilon_{Vn,h} \qquad (10)$$

Where $k_{Vp,h}(k–1)$ and $k_{Vn,h}(k–1)$ positive and negative sequences gains at instant k–1, respectively, and $\Delta k_{V,h}$ is the adaptive gain step.

The gain stabilizes automatically when the deviation between the voltages at instant k and *k-1* tends to zero. Furthermore, positive and negative sequence gains are limited to minimum ($k_{Vp,hMIN}$ and $k_{Vn,hMIN}$, respectively) and maximum values ($k_{Vp,hMAX}$ and $k_{Vn,hMAX}$, respectively), since high gain values can lead to system instability. Equations (11) and (12) shows the positive and negative sequence gains limitations, respectively and Fig. 2 shows the flowchart of the adaptive gains update algorithm.

$$k_{Vp,h} = \begin{cases} k_{Vp,hMIM} & if\ k_{Vp,h}(k) < k_{Vp,hMIM} \\ k_{Vp,hMAX} & if\ k_{Vp,h}(k) > k_{Vp,hMAX} \\ k_{Vp,h}(k) & otherwise \end{cases} \qquad (11)$$

$$k_{Vn,h} = \begin{cases} k_{Vn,hMIM} & if\ k_{Vn,h}(k) < k_{Vn,hMIM} \\ k_{Vn,hMAX} & if\ k_{Vn,h}(k) > k_{Vn,hMAX} \\ k_{Vn,h}(k) & otherwise \end{cases} \qquad (12)$$

IV. Modified IEEE 33-bus System

To validate the proposed control in a system with multiple buses, a modified version of the IEEE 33-bus system was proposed with the insertion of eight three-phase rectifiers and eight inverters with the proposed control in the system buses.

The number of power electronics-based devices is limited by the hardware-in-the-loop (HIL) setup used in the work. Fig. 3 shows an overview of the simulated system. In configuration 1, switches S1 and S2 are closed and switches S3 and S4 are open. In configuration 2, switches S1 and S2 are open and switches S3 and S4 are closed.

The modified IEEE 33-bus system was simulated in real-time in a multi-HIL configuration for HIL602 devices connected to a single computer using direct USB connection. HIL parallelism allows the connection of multiple devices of the same type into a single functional device with increased processing power and more inputs and outputs signals. Thus, it is possible to simulate larger and more complex systems with a greater presence of power electronics-based devices, such as rectifiers and static power converters. The modified IEEE 33-bus system was divided into four sub-circuits and each sub-circuit was allocated to a HIL602 device (device 1 to 4, as presented in Fig. 4). Also, four dual-core Texas Instruments' DSP TMSF28379D was used to implement VSG and harmonic damping controls proposed in this work. Each DSP is connected to one HIL device through a HIL TI DSP 180 Interface Card, meanwhile each core of every single dual-core DSP is responsible with the proposed VSG and harmonic damping controls for each inverter inserted in the system.

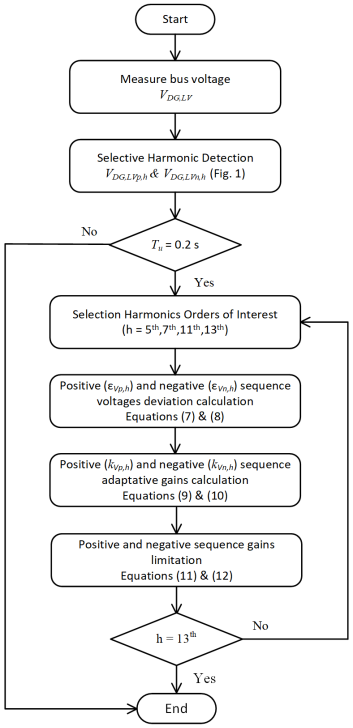

Fig. 2 - Flowchart of the adaptive gains update algorithm

Furthermore, each sub-circuit was partitioned to obtain the smallest possible time step in the simulation (4.0 µs). Configuration id 2 was adopted in this work, since this configuration has the largest number of standard processing cores (SPC) available (6 cores for each device, as presented in Fig. 4) and, consequently, allows the addition of more power electronics-based devices. With this configuration it was possible to insert eight non-linear loads (three-phase rectifiers) and eight inverters into the system. Fig. 4 shows the electrical and device partitioning in the proposed modified IEEE 33-bus systems and Table I shows where the inverters are connected.

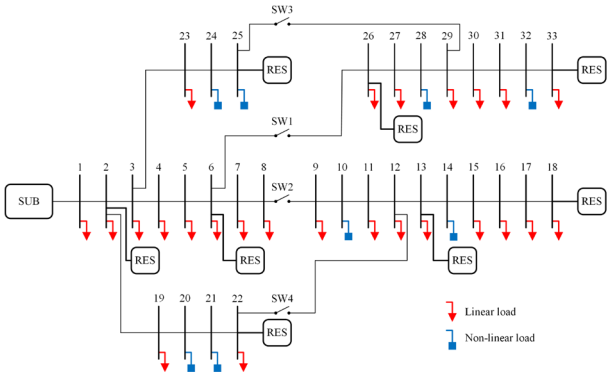

Fig. 3 - Modified IEEE 33-bus system

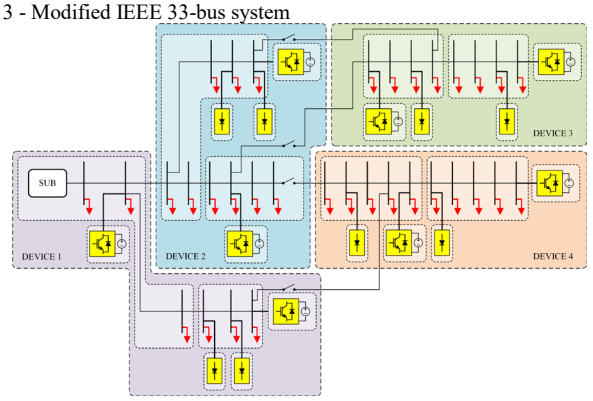

Fig. 4 - Partitioning of the modified IEEE 33-bus system in the setup with 4 HIL602 in parallel

TABLE I
CONNECTION OF INVERTERS IN THE MODIFIED IEEE 33-BUS SYSTEM

Inverter	Bus	HIL602 device
INV1	22	1
INV2	25	2
INV3	33	3
INV4	18	4
INV5	2	1
INV6	6	2
INV7	26	3
INV8	13	4

V. RESULTS

To evaluate the results of harmonic compensation and the improvement of the voltage profile at the fundamental frequency, due to harmonic damping and the VSG active power injection into the network, respectively, the sequence of addition of inverters into the grid is shown in Table II.

TABLE II
ORDER IN WHICH INVERTERS ARE CONNECTED TO THE GRID

Number of inverters	Inverters connected	
	IEEE 33-Bus 1	IEEE 33-Bus 2
1	1	4
2	1, 2	4, 3
3	1, 2, 3	4, 3, 2
4	1, 2, 3, 4	4, 3, 2, 1
5	1, 2, 3, 4, 5	4, 3, 2, 1, 8
6	1, 2, 3, 4, 5, 6	4, 3, 2, 1, 8, 7
7	1, 2, 3, 4, 5, 6, 7	4, 3, 2, 1, 8, 7, 6
8	1, 2, 3, 4, 5, 6, 7, 8	4, 3, 2, 1, 8, 7, 6, 5

Fig. 5 shows connection of the inverter with the proposed control strategy in a distribution system. The parameters of the inverter and the transformer used to connect the inverter to the

grid are shown in Tables III and IV, respectively. Table V shows the minimum and maximum gains and the adaptive gain step.

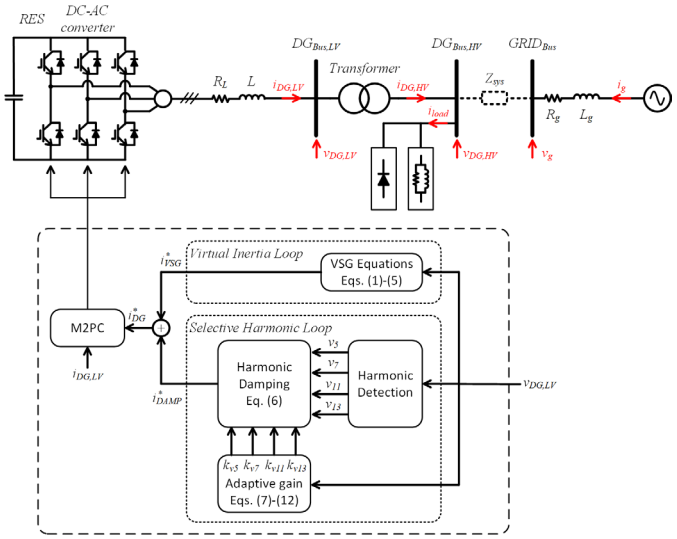

Fig. 5 - Application of DG with the proposed control in a multi-bus system

TABLE III
INVERTER PARAMETERS

Parameter	Value
Switching frequency	10 kHz
Grid Frequency	60 Hz
Converter nominal power	750 kVA
DC-link voltage	1500 V
Inverter inductance	0.27 mH

TABLE IV
TRANSFORMER PARAMETERS

Parameter	Value
Nominal power	1 MVA
Nominal frequency	60 Hz
Primary line-to-line voltage	12.66 kV
Secondary line-to-line voltage	480 V
Positive sequence short-circuit voltage	5 %
Positive sequence short-circuit losses	12.1 kW

TABLE V
ADAPTIVE GAIN PARAMETERS

Parameter	Value
Positive sequence minimum gain ($k_{Vp,hMIN}$)	-100
Positive sequence maximum gain ($k_{Vp,hMAX}$)	0
Negative sequence minimum gain ($k_{Vn,hMIN}$)	-100
Negative sequence maximum gain ($k_{Vn,hMAX}$)	0
Adaptive gain step for inverters 1, 2, 7, and 8 ($\Delta k_{V,h}$)	1
Adaptive gain step for inverters 3, 4, 5, and 6 ($\Delta k_{V,h}$)	2

Since MPPT control is not the focus of this study, it is assumed that the system's active and reactive powers are constant and equal to 500 kW and 0 kvar, respectively, which corresponds to 66.7% of the nominal inverter power. Therefore, due to the residual capacity available in the DG inverters, it is possible to implement ancillary services, such as compensation of harmonic voltages and currents.

A Modulated Model Predictive Control (M2PC) [26][27] is applied to the current control loop in the grid-tied inverter with an L filter. The choice of the L filter was due to the justification of the use of the M2PC to control the current loop of the inverters, since the mathematical model of the L filter is simpler than the LCL filter model, for example.

A total of 18 real-time simulations, 9 for each system configuration, were performed to show the influence of adding more DGs in order to analyze the influence of the adaptative harmonic damping control and the VSG control on the system THD reduction and the regulation of the fundamental component of the voltage in the system, respectively.

A. Selective harmonic damping

The percentage reduction in voltage THD after the insertion of inverters into the system is always calculated in relation to the voltage THD of the system without inverters.

Fig. 6 shows the voltage THD on each bus according to the sequential insertion of the eight inverters in both configurations of the modified IEEE 33-bus system.

In configuration 1, after the insertion of INV1 on bus 22, the voltage THD was practically unchanged in section 19-22, but it was reduced on bus 25 by 3.0%. Connecting INV1 does not significantly change the THD on the other system buses. The connection of INV2 on bus 25 causes a 20.2% reduction in the THD of bus 25 and a reduction on buses closer to bus 25, such as buses 23 and 24. The addition of INV3 on bus 33 causes the THD to be significantly reduced on the 26-33 section, with a reduction of 39.1 % on bus 33. The INV3 also reduces the THD in the 1-18 section, with a maximum reduction of 8.6% on the bus 18. The INV4 also reduces the voltage THD in section 26-33, since this section is connected to bus 6 of section 1-18. The insertion of INV5 in bus 2 causes a significant reduction in the main section of the network, since this inverter is close to four of the eight non-linear loads inserted in the system, despite being closer to the substation. A 62.6% THD reduction is observed on the bus 18 with the addition of INV5. The addition of INV6 on bus 6 slightly reduces THD on bus 1-18 and 26-33, with a maximum reduction of 63.1% on bus 18. The insertion of INV7 on bus 26 causes the THD in section 29-33 to have a greater reduction, with a reduction from 42.8% to 48.8% on bus 26, when compared with the THD for the system with six inverters.

In configuration 2, when INV4 is inserted on bus 18, the THD on this bus is drastically reduced, which lowers 47.7 % on bus 18. In addition to significantly reducing THD in section 9-18, there is also a notable reduction in section 20-22, which in this configuration is connected to section 9-18 via bus 12. The addition of INV3 on bus 26 reduced THD on the 26-33 section, with a maximum reduction of 44.0% on bus 33. A reduction can also be observed in section 23-25, which is connected to section 26-33 via bus 29, and section 1-8. In sections 23-25 and 1-8, maximum THD reductions of 19.6% on bus 25 and 17.6% on bus 2 were achieved, respectively. The connection of INV2 to bus 25 reduces the THD in sections 23-25 and 26-33, which is connected to section 23-25 through bus 29, and in section 1-8. The largest reduction observed in the 23-25 section after the insertion of INV2 is 34.1 % on the bus 25. The insertion of INV1 on bus 22 reduces the THD in the adjacent regions, which comprise sections 20-22 and 9-18, which is connected to section 20-22 through bus 22. The maximum reduction of 50.7% is observed on bus 18. The INV8 is connected to bus 13 and a maximum THD reduction of 58.0% is observed on bus 18 from section 9-18. A reduction of 33.9% is observed on bus 22 from the 20-22 section. The addition of INV7 to bus 26

significantly reduces THD on sections 23-25 and 26-33, with a 54.8% reduction on bus 26. A reduction in THD is also observed in section 1-8. The connection of INV5 to bus 2 only slightly changes the THD in sections 1-8 and 23-25, with a reduction of 44.8% in section 6-8. Connecting INV5 to node 2 only slightly changes the THD on the sections 23-25 and 26-33.

In both configurations, adding an eighth inverter to the system slightly deteriorated the THD on some buses. The performance of the harmonic voltage damping control with six, seven and eight inverters were similar in both configurations of the IEEE 33-bus system, with cases in which the system with eight inverters presented slightly worse results than those obtained with the systems with six or seven inverters.

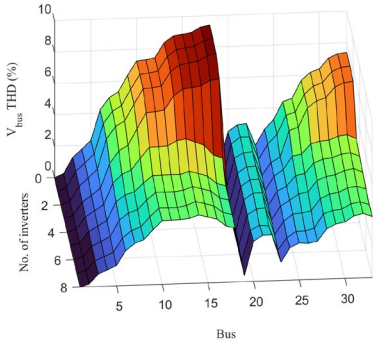

(a)

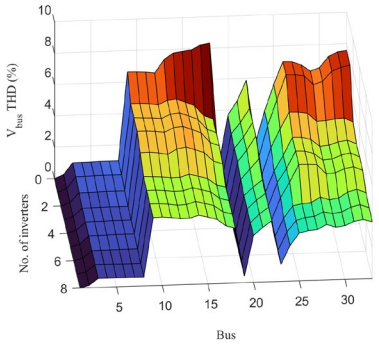

(b)

Fig. 6 - Voltage THD in the modified IEEE 33-bus system according to the number of inverters connected in the system: a) configuration 1 and b) configuration 2

Tables VI and VII show the V_{bus} THD reduction when the THD of each scenario with inverters are compared to the scenario without inverters in both configurations of the modified IEEE 33-bus system.

In configuration 1, the system with seven inverters achieves a maximum reduction of 63.6 % of the V_{bus} THD at node 718. In configuration 2, the system with seven inverters achieves a maximum reduction of 57.9 % of the V_{bus} THD at node 718. The system THD tends to decrease until the seventh and sixth inverters are added to the system in configuration 1 and 2, respectively, as can be seen in Table VI and VII. When the eighth is inserted in configuration 1, the THD slightly increases in some system buses. The insertion of the seventh and eighth inverters in configuration 2 doesn't significantly change the system THD. However, the system THD tends to remain stable in both configurations with the insertion of more inverters.

TABLE VI
THD REDUCTION ON SELECTED BUSES OF THE MODIFIED IEEE 33-BUS SYSTEM (CONFIGURATION 1)

No. of inv.	V_{bus} THD reduction (%)						
	6	13	18	22	25	26	33
1	0.0	0.1	0.0	0.7	-3.0	0.0	0.0
2	-2.4	-1.2	-1.1	-1.5	-20.2	-2.3	-1.4
3	-19.0	-9.2	-8.6	-2.8	-17.7	-19.7	-39.1
4	-28.0	-32.8	-53.2	-1.7	-24.0	-28.2	-42.4
5	-35.1	-48.3	-62.6	-1.7	-24.3	-35.0	-44.4
6	-42.5	-49.8	-63.1	-4.8	-24.8	-42.8	-47.0
7	-48.9	-51.0	-63.6	-13.5	-31.7	-48.8	-48.8
8	-47.4	-50.4	-63.5	-3.7	-27.6	-47.1	-47.2

TABLE VII
THD REDUCTION ON SELECTED BUSES OF THE MODIFIED IEEE 33-BUS SYSTEM (CONFIGURATION 2)

No. of inv.	V_{bus} THD reduction (%)						
	6	13	18	22	25	26	33
1	-1,6	-23,6	-47,7	-15,9	-1,8	0,5	-0,8
2	-17,1	-23,6	-47,7	-16,0	-19,6	-21,1	-37,2
3	-28,4	-23,5	-47,3	-15,9	-34,1	-31,6	-44,0
4	-29,1	-30,2	-50,7	-25,8	-33,8	-31,7	-43,6
5	-30,3	-42,7	-58,0	-33,9	-33,5	-31,5	-43,4
6	-38,5	-42,6	-57,8	-33,9	-45,0	-54,8	-50,6
7	-44,8	-42,6	-57,6	-33,9	-46,4	-54,8	-51,9
8	-43,8	-42,7	-57,9	-33,6	-45,0	-54,4	-52,2

Fig. 7 displays the THD profile across the 33 system buses in both configurations for the purpose of analyzing the THD profile throughout the distribution system as the inverters are connected to the grid.

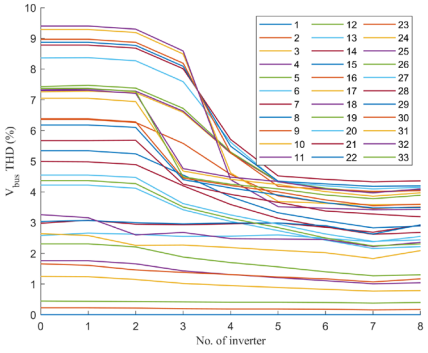

(a)

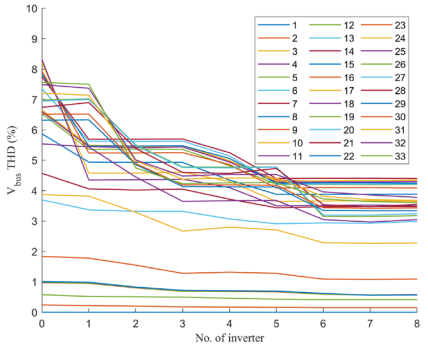

(b)

Fig. 7 – THD in the IEEE-33 bus system with the gradual connection of the eight inverters in the system: a) configuration 1 and b) configuration 2

The THD behavior of the selected buses in Tables VI and VII is comparable to the THD behavior of the overall system as seen in Fig. 7. In Fig. 7(a), the system THDs are at their minimum when seven inverters are connected to the system. After the eighth inverter is connected, the THDs of the system

buses increase slightly, but the system THDs tend to remain constant. In Fig. 7(b), the system THDs reach minimum values in simulations with six or more inverters and, after the connection of the sixth inverter, the THD tends to remain constant. Due to the limits of the real-time simulation system, which consisted of four HIL602 devices connected in parallel, simulations using nine or more inverters were not feasible. However, independent of system configuration, the use of five or more inverters can mitigate the grid THD to values below 5 %, as proposed by IEEE Std. 519-2022 [28] validating the effectiveness of the proposed adaptative harmonic mitigation with multiple inverters even without communication between them.

B. Voltage profile in the fundamental component

Fig. 8 shows the fundamental component of the voltage on each bus according to the sequential activation of the eight inverters in both configurations of the modified IEEE 33-Bus System.

In configuration 1, the voltage profile near the buses where the DGs are situated is improved by the installation of inverters INV1, INV2, INV3, and INV4 on buses 22, 25, 33, and 18, respectively. Since inverters INV5 and INV6 are placed at a location in the network where many high-power loads are present, connecting them to buses 2 and 6, respectively, greatly enhances voltage regulation across the system. The INV7 is connected to bus 26, significantly improving the voltage profile in sections 26-33 and in section 1-18, which is connected to section 26-33 via bus 6. The addition of INV8 on bus 13 practically does not change the system voltage profile.

In configuration 2, the addition of INV4 on bus 18 improves the voltage profile on sections 9-18 and 19-22, since these sections are connected through buses 22 and 12. The connection of INV3 visibly improves the voltage profile in sections 23-25 and 26-33, since this inverter is connected to section 26-33 via bus 29. The addition of INV2 on bus 25 improves voltage on sections 23-25 and 26-33 and slightly improves voltage on sections 1-8. The insertion of INV1 on bus 22 significantly improves the voltage profile on sections 19-22 and 9-18 of the IEEE 33-Bus system - configuration 2, since it is installed close to high-power loads. The addition of INV8 on bus 13 significantly improves the voltage profile on sections 9-18 and 19-22 e the connection of INV7 to bus 26 significantly increases the voltage on the fundamental component in sections 23-25 and 26-33. The insertion of INV6 improves the voltage profile in section 1-8, since this inverter is connected to bus 6. The IEEE 33-Bus system's voltage profile in configuration 2 remains unchanged when INV5 is added to bus 2. Notably, following the installation of inverters INV7, INV6, and INV5, the voltage profile in sections 9-18, 19-22, 23-25, and 26-33 essentially remains same.

Table VIII and IX show the V_{bus} of scenarios with inverters and without inverters in both configurations of the modified IEEE 33-bus system.

The voltages on all system buses are always greater than 0.95 p.u. for systems with six or more inverters in both configurations. In the worst-case scenario on bus 718, the system voltage went from 0.899 p.u. to 0.965 (7.37 %) and went from 0.930 p.u. to 0.976 (4.87%) in configurations 1 and 2, respectively.

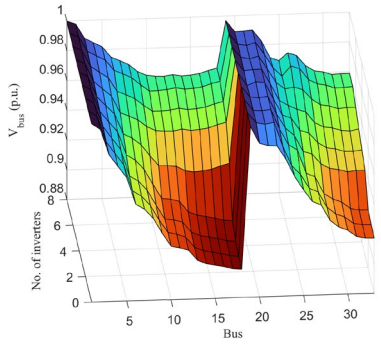

(a)

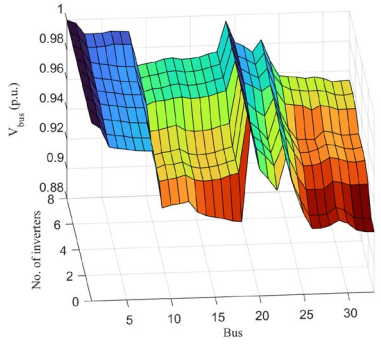

(b)

Fig. 8 - Voltage regulation in the modified IEEE 33-bus system according to the number of inverters connected in the system: a) configuration 1 and b) configuration 2

TABLE VIII
VOLTAGE REGULATION ON SELECTED BUSES OF THE MODIFIED IEEE 33-BUS SYSTEM (CONFIGURATION 1)

No. of inv.	V_{bus} (p.u.)						
	6	13	18	22	25	26	33
0	0.945	0.906	0.899	0.981	0.951	0.943	0.917
1	0.945	0.906	0.899	0.988	0.953	0.943	0.917
2	0.947	0.908	0.900	0.988	0.961	0.945	0.919
3	0.952	0.913	0.906	0.989	0.962	0.951	0.937
4	0.958	0.932	0.936	0.989	0.965	0.956	0.942
5	0.963	0.951	0.955	0.990	0.965	0.962	0.947
6	0.969	0.956	0.960	0.990	0.967	0.968	0.953
7	0.975	0.962	0.965	0.990	0.967	0.974	0.958
8	0.975	0.962	0.965	0.990	0.969	0.974	0.959

TABLE IX
VOLTAGE REGULATION ON SELECTED BUSES OF THE MODIFIED IEEE 33-BUS SYSTEM (CONFIGURATION 2)

No. of inv.	V_{bus} (p.u.)						
	6	13	18	22	25	26	33
0	0.980	0.938	0.930	0.951	0.934	0.924	0.921
1	0.980	0.951	0.954	0.958	0.935	0.924	0.921
2	0.982	0.951	0.955	0.958	0.942	0.933	0.936
3	0.983	0.951	0.955	0.959	0.949	0.940	0.943
4	0.984	0.958	0.962	0.966	0.950	0.941	0.943
5	0.984	0.972	0.975	0.974	0.949	0.941	0.943
6	0.985	0.972	0.975	0.974	0.956	0.956	0.952
7	0.992	0.972	0.976	0.975	0.960	0.957	0.953
8	0.992	0.972	0.976	0.975	0.958	0.957	0.953

VI. CONCLUSIONS

The proposed decentralized and selective control with adaptive gain for harmonic voltage damping can improve the harmonic content of the modified IEEE 33-bus system. Furthermore, the insertion of DGs also improves the voltage

profile of the system under study.

In both configurations of the modified IEEE 33-bus system, as shown in Tables VI and VII, the THD decreases gradually by adding the inverters until INV7 is inserted into the system. When compared to the system with seven inverters, the addition of INV8 slightly worsens harmonic mitigation. However, Fig. 7 shows that the system voltage THDs tends to remain constant validating the effectiveness of the proposed adaptative harmonic mitigation with multiple inverters. In configuration 1, the system with seven inverters achieves a maximum reduction of 63.6 % of the V_{bus} THD at node 718. In configuration 2, the system with seven inverters achieves a maximum reduction of 57.9 % of the V_{bus} THD at node 718. The use of five or more inverters in both system configurations can mitigate the grid THD to values below 5 %, as proposed by IEEE 519-2022 standard.

As shown in Tables VIII and IX, the multi-bus system's voltage regulation is greatly enhanced by the penetration of DGs throughout the system. When compared to voltages in the system without DGs, the distribution of DGs throughout the system reduces system voltage drops, increasing bus voltages. In configurations 1 and 2, bus 18 had the lowest voltage in the system; after the DGs were added, the voltages at this node rose by 7.37 % and 4.87 %, respectively.

The proposed decentralized control with adaptive gain can mitigate the whack-a-mole effect that can occur with the application of decentralized controls and is a technically and financially viable option for systems in which centralized or distributed controls with communication cannot be applied, due to the absence of a communication system.

VII. References

[1] Fernando M. Camilo, V. Fernão Pires, Rui Castro, M.E. Almeida, The impact of harmonics compensation ancillary services of photovoltaic microgeneration in low voltage distribution networks, Sustainable Cities and Society, Volume 39, 2018, Pages 449-458.

[2] Y. W. Li and J. He, "Distribution System Harmonic Compensation Methods: An Overview of DG-Interfacing Inverters," in IEEE Industrial Electronics Magazine, vol. 8, no. 4, pp. 18-31, Dec. 2014.

[3] Yahya Naderi, Seyed Hossein Hosseini, Saeid Ghassem Zadeh, Behnam Mohammadi-Ivatloo, Juan C. Vasquez, Josep M. Guerrero, An overview of power quality enhancement techniques applied to distributed generation in electrical distribution networks, Renewable and Sustainable Energy Reviews, Volume 93, 2018, Pages 201-214.

[4] Selcuk Sakar, Murat E. Balci, Shady H.E. Abdel Aleem, Ahmed F. Zobaa, Integration of large- scale PV plants in non-sinusoidal environments: Considerations on hosting capacity and harmonic distortion limits, Renewable and Sustainable Energy Reviews, Volume 82, Part 1, 2018, Pages 176-186.

[5] A. Costabeber, P. Tenti, T. Caldognetto and E. V. Liberado, "Selective compensation of reactive, unbalance, and distortion power in smart grids by synergistic control of distributed switching power interfaces," 2013 15th European Conference on Power Electronics and Applications (EPE), Lille, France, 2013, pp. 1-9.

[6] G. Pepermans, J. Driesen, D. Haeseldonckx, R. Belmans, W. D'haeseleer, Distributed generation: definition, benefits and issues, Energy Policy, Volume 33, Issue 6, 2005, Pages 787-798.

[7] Lucas Frizera Encarnação, Daniel Carletti, Sabrina de Angeli Souza, Odair de Barros Jr., Dayane Corneau Broedel, Patrick Trivilin Rodrigues, 11 - Virtual Inertia for Power Converter Control, Editor(s): Imene Yahyaoui, Advances in Renewable Energies and Power Technologies, Elsevier, 2018, Pages 377-411.

[8] H. -P. Beck and R. Hesse, "Virtual synchronous machine," 2007 9th International Conference on Electrical Power Quality and Utilisation, Barcelona, Spain, 2007, pp. 1-6.

[9] K. Visscher and S. W. H. De Haan, "Virtual synchronous machines (VSG's) for frequency stabilisation in future grids with a significant share of decentralized generation," CIRED Seminar 2008: SmartGrids for Distribution, Frankfurt, 2008, pp. 1-4.

[10] L. Lin, Q. Jia, C. Lv, J. Liang and P. Luo, "Partitional Collaborative Mitigation Strategy of Distribution Network Harmonics Based on Distributed Model Predictive Control," in IEEE Transactions on Smart Grid, vol. 14, no. 3, pp. 1998-2009, May 2023, doi: 10.1109/TSG.2022.3211008.

[11] H. Zhai et al., "An Optimal Compensation Method of Shunt Active Power Filters for System-Wide Voltage Quality Improvement," in IEEE Transactions on Industrial Electronics, vol. 67, no. 2, pp. 1270-1281, Feb. 2020.

[12] Munir, Hafiz Mudassir, Jianxiao Zou, Chuan Xie, and Josep M. Guerrero. 2019. "Cooperation of Voltage Controlled Active Power Filter with Grid-Connected DGs in Microgrid" Sustainability 11, no. 1: 154.

[13] T. -L. Lee, P. -T. Cheng, H. Akagi and H. Fujita, "A Dynamic Tuning Method for Distributed Active Filter Systems," in IEEE Transactions on Industry Applications, vol. 44, no. 2, pp. 612-623, March-april 2008.

[14] H. K. Morales-Paredes, J. P. Bonaldo and J. A. Pomilio, "Centralized Control Center Implementation for Synergistic Operation of Distributed Multifunctional Single-Phase Grid-Tie Inverters in a Microgrid," in IEEE Transactions on Industrial Electronics, vol. 65, no. 10, pp. 8018-8029, Oct. 2018, doi: 10.1109/TIE.2018.2801780.

[15] Thiago Silva Amorim, Odair de Barros, Daniel Carletti, Lucas Frizera Encarnação, Inverter Controller with Synthetic Inertia and Adaptive Harmonic Damping Based on Fourier Linear Combiners, Electric Power Systems Research, Volume 223, 2023, 109660.

[16] A. Das, A. Shukla, A. B. Shyam, S. Anand, J. M. Guerreo and S. R. Sahoo, "A Distributed-Controlled Harmonic Virtual Impedance Loop for AC Microgrids," in IEEE Transactions on Industrial Electronics, vol. 68, no. 5, pp. 3949-3961, May 2021.

[17] A. Shukla, A. Das and S. Anand, "Method to Reduce Harmonic Voltage Distortion and Improve Harmonic Current Sharing in an islanded AC Microgrid," 2019 IEEE International Conference on Industrial Technology (ICIT), Melbourne, VIC, Australia, 2019, pp. 498-503.

[18] J. Chen et al., "Distributed Control of Multi-Functional Grid-Tied Inverters for Power Quality Improvement," in IEEE Transactions on Circuits and Systems I: Regular Papers, vol. 68, no. 2, pp. 918-928, Feb. 2021.

[19] T. -T. Nguyen and H. -M. Kim, "Cluster-Based Predictive PCC Voltage Control of Large-Scale Offshore Wind Farm," in IEEE Access, vol. 9, pp. 4630-4641, 2021.

[20] Mousavi, Seyyed Yousef Mousazadeh, et al. "Coordinated control of multifunctional inverters for voltage support and harmonic compensation in a grid-connected microgrid." Electric Power Systems Research 155 (2018): 254-264.

[21] M. E. Baran and F. F. Wu, "Network reconfiguration in distribution systems for loss reduction and load balancing," in IEEE Transactions on Power Delivery, vol. 4, no. 2, pp. 1401-1407, April 1989.

[22] Y. Chen, R. Hesse, D. Turschner and H. -P. Beck, "Improving the grid power quality using virtual synchronous machines," 2011 International Conference on Power Engineering, Energy and Electrical Drives, Malaga, Spain, 2011, pp. 1-6.

[23] P. Rodriguez, A. Luna, M. Ciobotaru, R. Teodorescu and F. Blaabjerg, "Advanced Grid Synchronization System for Power Converters under Unbalanced and Distorted Operating Conditions," IECON 2006 - 32nd Annual Conference on IEEE Industrial Electronics, Paris, France, 2006, pp. 5173-5178.

[24] H. Akagi, E.H. Watanabe, M. Aredes, Instantaneous Power Theory and Applications to Power Conditioning, John Wiley & Sons, New Jersey, 2007. IEEE Press Series on Power Engineering.

[25] IEEE Recommended Practice for Monitoring Electric Power Quality, IEEE Std 1159-2019 (Revision of IEEE Std 1159-2009), pp.1-98, 13 Aug. 2019.

[26] M. Rivera et al., "A modulated model predictive control scheme for a two-level voltage source inverter," 2015 IEEE International Conference on Industrial Technology (ICIT), Seville, Spain, 2015, pp. 2224-2229.

[27] BV Comarella, D Carletti, I Yahyaoui, LF Encarnação. Theoretical and Experimental Comparative Analysis of Finite Control Set Model Predictive Control Strategies. Electronics. 2023; 12(6):1482.

[28] IEEE Standard for Harmonic Control in Electric Power Systems, IEEE Std 519-2022 (Revision of IEEE Std 519-2014), pp.1-31, 5 Aug. 2022.